

## OPTICAL AND ELECTRICAL CHARACTERIZATION OF SiC DEVICES

Ryne P. Raffaele, Rochester Institute of Technology, Rochester, New York 14623  
Sheila G. Bailey, Phillip Neudeck, and Robert Okojie, NASA Glenn Research Center, Cleveland, OH 44135  
C.M. Schnabel and M. Tabib-Azar, Case Western Reserve University, Cleveland, OH 44106  
Dave Scheiman and Phillip Jenkins, Ohio Aerospace Institute, Cleveland, OH 44137  
Seth Hubbard, Univ. of Michigan, Ann Arbor, MI 41809

### ABSTRACT

The semiconductor SiC has long been known for its outstanding resistance to harsh environments (e.g., thermal stability, radiation resistance, dielectric strength). However, the ability to produce device quality material is severely limited by the inherent crystalline defects associated with this material and their associated electronic effects. Much progress has been made recently in the understanding and control of these defects and in the improved processing of this material. This work has made the possibility of producing SiC based solar cells for high-temperature, high-light intensity, and high-radiation missions, such as experienced by solar probes. In this paper, we will present our recent studies on defects in SiC and the synthesis and characterization SiC based solar cells.

### INTRODUCTION

The ability to identify the electrical properties of crystal defects in semiconductors is essential in developing the appropriate material qualities for future devices. This role is particularly important in the development of SiC as a photovoltaic material. The 6H-SiC polytype is a promising wide bandgap ( $E_g = 3.0$  eV) semiconductor which is being developed for use in high-temperature, high-power, high-frequency, and high-radiation conditions [1]. The advantages of this material lie in its extremely large breakdown field strength, high thermal conductivity, good electron saturation drift velocity, and stable electrical performance at temperatures as high as 600 °C [2]. These properties have made SiC an ideal candidate for high-temperature electronics and high-power microwave devices. In addition, it has also generated interest in the space power community as a possible photovoltaic solar cell material for devices capable of operating within three solar radii of the sun [3].

The processing techniques required to produce high-quality SiC wafers has undergone tremendous improvement since this material was first investigated for semiconductor applications. However, even the best SiC produced today still has a large density of crystallographic defects [4]. The most prominent of these defects being screw-dislocations and their hollow-core counterparts, micropipes [5]. These defects have been correlated with increased reverse leakage currents and reverse bias breakdown in SiC Schottky diodes [6].

In order to better characterize these defects and understand their role in the electronic performance of SiC-based devices, Schottky barriers on 6H-SiC epilayers have been analyzed by a variety of electrical and structural characterization techniques. An effort has been made to correlate the structural defects, specifically screw dislocations, with electronic recombination centers.

The structural defects have been investigated using synchrotron white-beam X-ray topography. This technique produces a gray-scale image that identifies regions of stress within the crystalline lattice. Surface imperfections have also been examined using Nomarski microscopy and atomic force microscopy. Nomarski microscopy uses the interference of converging beams of light to be able to identify surface features and atomic step heights as small as 30 angstroms [7]. Atomic force microscopy is an ultra-low force profilometer capable of measuring height differences on the atomic scale.

The electronic recombination centers have been identified using electron-beam induced current (EBIC) measurements. EBIC is performed in a scanning electron microscope (SEM). In this technique, as the electron beam in the SEM is rastered across the surface, the current induced in the device by the creation of electron-hole pairs at or near the boundary depletion width is measured [8]. The induced current is then plotted in gray-scale as a function of beam position. Areas in which there is significant carrier recombination and low induced current appear darker in the resulting image.

In association with our materials studies, we have also produced and measured the first SiC-based solar cells. Both n on p and p on n cells were fabricated. The photoresponse of these cells under 1 sun AM0 illumination at room temperature and at elevated temperatures under a 150 sun concentration was measured.

### EXPERIMENTAL PROCEDURE

6H-SiC schottky barrier diodes were made by growing a 3.0 mm thick homoepilayer on 3.5° off-axis n-type SiC wafers obtained from Cree Research, Inc. The samples were nitrogen doped to  $10^{16}$  cm<sup>-3</sup> during epilayer growth. Immediately following a surface clean-up using a buffered HF etch and rinse, 40 nm thick gold contacts were electron beam evaporated and patterned into 0.9 mm square pads using lift-off photolithography.

SiC solar cells were made using n on p and p on n wafers obtained from Cree Research, Inc. The wafers were first rapid thermal annealed at 1000 °C for 2 minutes in an argon atmosphere. They were then cleaned first in acetone (5 min. hot) and in isopropyl alcohol (1 min.), and then dehydrated at 130 °C for 3 min. on a hotplate. A spin coater was then used to spin at 4.5 Krpm for 30 s as HMDS was applied. They were then spun at 4.5 Krpm for 30 s as PRS 1813 photoresist was applied. The samples were then heated on a hotplate at 105 °C for 1 minute. The sample and our solar cell grid pattern mask (0.48 cm<sup>2</sup>) were then placed in a precision aligner and exposed to UV radiation. The photoresist was then developed and etched. The grid was then produced by a series of metal evaporations. These were in order: Ti, Al, Au, Pt with thicknesses of 50, 1000, 1000, and 200 angstroms, respectively (see Figure 1). The grid patterning was then finalized by etching in acetone (see Figure 2). Two different contact annealing routines were used for both types of cells. The first was 35 s at 900 °C in argon. The second was 2 min. at 800 °C in argon. The cells were finished by evaporatively coating them with Al and then gold at 1000 and 2000 angstroms, respectively.

The structural defects in the 6H-SiC were analyzed using synchrotron white-beam X-ray topography (SWBXT) at NSLS at Brookhaven National Lab. Surface defects were imaged using Nomarski microscopy and a Digital Instruments Nanoscope III atomic force microscope (AFM). The electrical behavior of the Schottky diodes was analyzed using current versus voltage and capacitance versus voltage measurements using a computer controlled Keithley 236 Source/Measure Unit and a Keithley 590 CV Analyzer. Electronic defects in the diodes and solar cells were imaged using electron-beam induced current (EBIC) measurements performed in a Hitachi S-800 Field-Emission Scanning Electron Microscope (SEM).

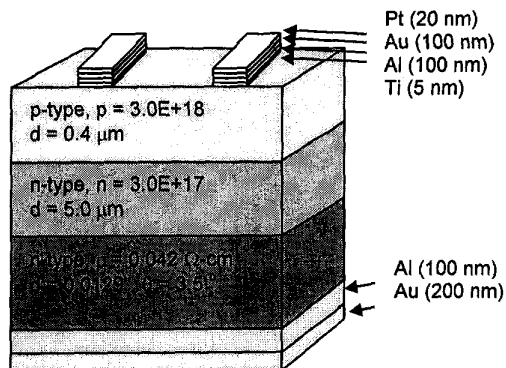


Figure 1. Cross-section schematic of the p on n SiC solar cell.

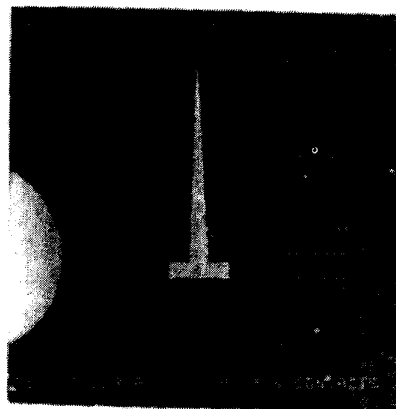


Figure 2. Photograph of n on p SiC solar cell.

The SiC solar cells were measured under a simulated AMO 1 sun source at room temperature. Presently, accurate calibration of these cells is not possible due to a lack of AMO calibrated SiC cell for comparison. In time, standard cells will become available but for now considerable guesswork was used to estimate conversion efficiency and AMO performance. Using an Spectrolab X-25 Xenon simulator set using a GaInP (~1.75eV) standard cell, the short circuit current was 0.2 mA. Measurements under concentration were made using a Spectrolab LAPSS system. A single tube flash simulator was focused using a 2" diameter CaF<sub>2</sub> lens. The solar intensity was estimated using a reference cell at the lens plane and applying simple optical concentration yielded a solar intensity of approximately 150 suns at the cell plane. The measured I<sub>sc</sub> of 45mA is nearly 225X that of the one sun current. Early indications are that this is a super linear effect in the cell's current collecting capability. This is not uncommon among solar cells. It is however, quite possible that the uncertainty in our calibration intensity is responsible for the apparent super linear nature of the cell.

## RESULTS AND DISCUSSION

The contrast in the SWBXT image represents areas of stress in the crystalline lattice. The image shown was digitally re-scaled to remove the asymmetric distortion associated with the SWBXT technique. The white spots appearing in the image are indicative of screw dislocations. EBIC was performed on the same area that is after it was coated with gold. Many dark areas corresponding to recombination centers or electronic defects at or near the metal semiconductor junction can be seen. A mask of the screw dislocations identified in the SWBXT image of the diodes was overlaid on the EBIC image (see Figure 3). It is evident from this result that the screw dislocations act as electronic recombination centers.

A Nomarski microscope was used to look at the surface imperfections on the same sample discussed above. The area was divided into 12 smaller sections

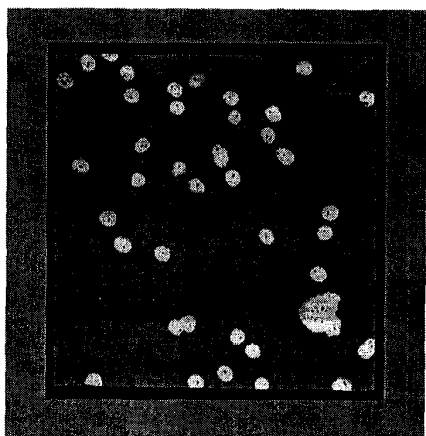


Figure 3. A Screw dislocation mask, from a SWBXT image, overlaid on an EBIC scan of a Au Schottky barrier placed on the same area. Dark spots in the EBIC scan correspond to electronic recombination centers and are found at each of the screw dislocations.

from which to obtain the high resolution Nomarski images. These images were then combined to produce the image of the entire area. Overlaying the same screw dislocation mask used in Figure 3 (generated using the SWBXT image) on the Nomarski image shows that screw dislocations also result in growth pits. Surface particulates were found at the locations in which screw dislocations were present and no growth pits were recorded. It is believed that the particulates may have obscured the growth pits in those areas. The growth pits that correspond to screw dislocations have a characteristic shape, as seen in the Nomarski images. Atomic force microscopy was used to investigate the topography of the screw dislocation growth pits. The current versus voltage scans of the Schottky barriers and pn junctions produced in this study showed good Shockley diode behavior. However, several of the diodes showed non-linear behavior in the Log current versus voltage forward bias scan (see Figure 4). This behavior has previously been reported in SiC Schottky diodes by Defives et. al. and has been attributed to a dual barrier height mode [9]. It is believed that junction defects give barrier height inhomogeneities, causing the device characteristics to resemble two barriers in parallel. This behavior did not correlate to the position of the die on the sample surface. This behavior also did not correlate with the number or type of electrical or structural defects identified in this study. The barrier heights obtained from the current versus voltage behavior of the various dies were between 0.85 and 1.08 eV. The ideality factors for all the diodes measured were between 1.1 and 1.5. The reverse-bias analysis of these Schottky diodes showed a wide variety of breakdown types and voltages. The types range from very soft to extremely hard and the voltages ranged from approximately 40 V to nearly 140 V. However, only a slight correlation between screw dislocation and premature breakdown was apparent.

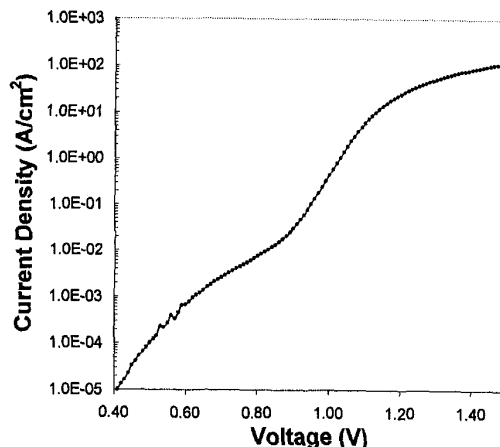


Figure 4. Non-linear current versus voltage behavior of SiC Schottky barriers.

Capacitance versus voltage measurements were performed on all the Schottky barriers to determine dopant densities as a function of position on the sample surface. The results were analyzed using a simple parallel-plate capacitor model [10]. These results were also used to investigate possible vertical dopant gradients within the epilayer. All of the dies showed excellent linearity in their inverse capacitance squared versus voltage behavior, indicating a homogenous vertical doping in the epilayer. The carrier densities for 5 different dies spread out uniformly over the sample surface were all with a range of  $1.12 \times 10^{16}$  to  $1.21 \times 10^{16} \text{ cm}^{-3}$ . These values are in good agreement with the anticipated doping density. The dies from which these values were obtained were randomly distributed across the sample surface and therefore did not indicate any transverse doping gradients across the sample. The barrier heights were between 1.2 and 1.3 eV.

The room temperature AM0 photoresponse of the different SiC solar cells was measured. The cells had poor open-circuit voltages and low short-circuit currents. However, not much photoresponse would be expected due to the lack of intensity in the solar spectrum above 3.0 eV. This first attempt at fabrication SiC cells yielded very low efficiencies. The results of the different cell types and annealing schemes is shown in Table 1. The cell performance was improved under concentration as shown in figure 5. The short-circuit current increased and the cell efficiency improved slightly as expected.

Cell Type	Temp (°C)	Area (cm <sup>2</sup> )	Isc (mA)	Voc (mV)	Fill
n on p	900	0.48	0.205	715.2	29.1
n on p	800	0.48	0.205	241.2	25.5
p on n	900	0.48	0.126	163.8	29.2
p on n	800	0.48	0.092	1245	15.9

Table 1. SiC solar cell AM0 performance.

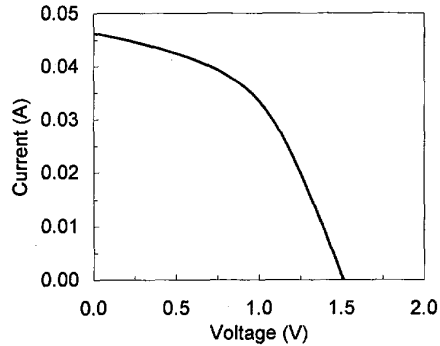


Figure 5. I-V photoresponse for a SiC solar cell in 150 suns measured at room temperature.

The temperature dependence of the SiC cells was measured in the 150 sun concentrated source. The thermal stability of a SiC solar cell would be expected to be quite good. A SiC solar cell should survive up to temperatures exceeding 1200 °C [3]. Unfortunately, the decrease in performance of these cells was greater than would be expected (see Figure 6). Much of the poor performance of these cells can be attributed to the grid contacts. SEM images of the contacts for both the n on p and p on n cells showed significant degradation with both annealing schemes (see Figures 7 & 8).

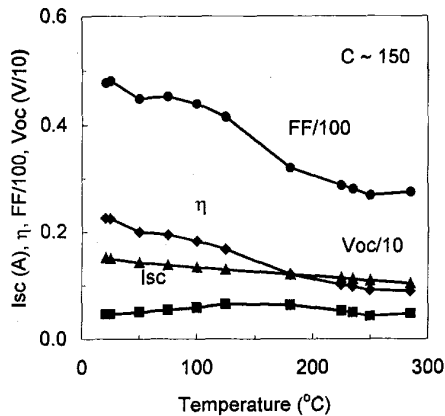


Figure 6.  $I_{sc}$ ,  $V_{oc}$ ,  $\eta$ , and FF vs. temperature under concentration of approximately 150 suns.

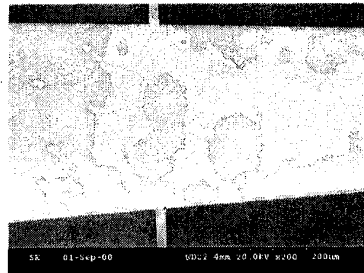


Figure 7. Micrograph of center grid line annealed at 900 °C for 35 s on a n on p SiC solar cell.

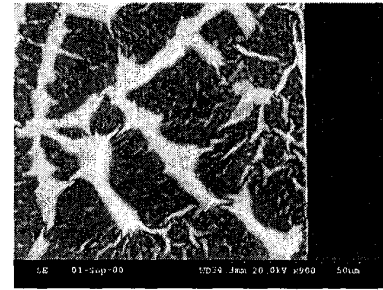


Figure 8. Micrograph of the center grid line annealed at 800 °C for 120 s on a p on n SiC solar cell.

## CONCLUSIONS

A correlation between screw dislocations and electronic recombination centers in SiC Schottky barriers has been shown. Nomarski microscopy showed that these screw dislocations result in growth pits on the semiconductor surface. The growth pits associated with screw dislocations have a characteristic shape identified by atomic force microscopy. The junctions analyzed by EBIC were shown to have numerous electronic defects, although most exhibited reasonable diode characteristics. The first ever SiC based solar cells were fabricated and measured. Optimization of the cell design and better contacting schemes should allow for the development of SiC solar cells that are well suited for future solar probe missions.

## REFERENCES

- [1] P.G. Neudeck, *J. Electron. Mater.* **24**, 283 (1995).
- [2] M. Bhatnagar and B.J. Baliga, *IEEE Trans. on Electron Devices* **40**, 645 (1993).
- [3] D.A. Scheiman, G.A. Landis, and V.G. Weizer, *Space Technology and Applications International Forum*, AIP Proc. **453** (1999).
- [4] P.G. Neudeck, W. Huang, and M. Dudley, in *Power Semiconductor Materials and Devices*, (MRS, Warrendale, PA 1998), Vol. 483, pp. 285-384.
- [5] P.G. Neudeck and J.A. Powell, *IEEE Electron Device Lett.* **15**, 63 (1994).
- [6] P.G. Neudeck, W. Huang, and M. Dudley, *IEEE Trans. Electron Devices* **46**, 478 (1999).
- [7] G. Nomarski, French Patents Nos. 1059124 and 1056361.
- [8] D.K. Schroder, *Semiconductor Material and Device Characterization* (John Wiley & Sons, NY, NY 1990), pp.391-394.
- [9] D. Defives, O. Noblanc, C. Dua, C. Brylinski, M. Barthula, V. Aubry-Fortuna, and F. Meyer, *IEEE Trans. on Electron Dev.* **46**, 449 (1999).
- [10] S.M. Sze, *Physics of Semiconductor devices* (John Wiley & sons, New York, 1981), 2<sup>nd</sup> edition, pp.248-249.